Carcinogenesis vol.23 no.1 pp.131–142, 2002

Induction of cytostasis in mammary carcinoma cells treated with the anticancer agent perillyl alcohol

Wenge Shi[2] and Michael N.Gould[1,3]

[1]McArdle Laboratory for Cancer Research, Department of Oncology, Room 506A, 1400 University Ave, Madison, WI 53706, USA

[2]Present address: Howard Hughes Medical Institute, Department of Cellular and Molecular Medicine, HHMI/CMM-West, Room 219, University of California-San Diego School of Medicine, Mail Code 0686, 9500 Gilman Drive, La Jolla, CA 92093-0686, USA

[3]To whom correspondence should be addressed
Email: gould@humonc.wisc.edu

The monoterpene perillyl alcohol (POH) has preventive and therapeutic effects in a wide variety of pre-clinical tumor models, including those for breast cancers, and is currently being tested in human phase I clinical trials. POH causes both cytostasis and apoptosis in rat mammary carcinomas. *In vitro*, POH inhibits cellular proliferation in a variety of mammalian cell lines. Here we investigated the mechanisms underlying cytostasis by studying the effects of POH on the cell cycle *in vitro* using the murine mammary transformed cell line TM6. In TM6 cells, POH causes an early G_1 cell-cycle block and slows the G_2–M transition. An increase in pRB in its hypophosphorylated state is associated with the early G_1 block caused by POH. POH treatment inhibits two important targets in the cells during the G_1–S transition: cyclin D1- and cyclin E-associated kinase. POH treatment leads to a reduction in cyclin D1 RNA and protein levels and prevents the formation of active cyclin D1-associated kinase complexes in synchronous cells during the exit of G_0 and entry into the cell cycle. In addition, POH treatment induces an increased association of $p21^{WAF1}$ with cyclin E–Cdk2 complexes, and inhibits the activating phosphorylation of Cdk2. All these effects of POH may contribute to the inhibition of the transition out of the G_1 phase of the cell cycle.

Introduction

Monoterpenes, including limonene and perillyl alcohol, are a class of phytochemical compounds that have both chemopreventive and therapeutic activities against a wide variety of experimental cancers including rat mammary cancers (1,2). Clinical trial results for perillyl alcohol demonstrated that monoterpenes have the potential of treating cancers without major toxicity (3–5). Further understanding their mechanisms of action may lead to the identification of more potent compounds in this class for the prevention and treatment of targeted cancer types.

The monoterpenes have been shown to have diverse cellular and molecular effects both *in vivo* and *in vitro*. The induction of hepatic phase I and phase II detoxifying enzymes by monoterpenes may underlie their blocking action at the initiation stage of chemical carcinogenesis (2,6,7). In addition, monoterpenes can modulate the mevalonate pathway at several points distal to HMG-CoA reductase, including inhibition of the isoprenylation of certain small G proteins (8–10), and inhibition of both the synthesis of ubiquinone and the conversion of lathosterol to cholesterol (11). Dietary monoterpene-induced tumor regression is associated with changes in the cellular level of several gene products, especially those involved in the transforming growth factor β (TGFβ) signaling pathway (12,13). For example, in regressing mammary carcinomas, monoterpene induced the expression of mannose 6-phosphate (M6P)/insulin-like growth factor II (IGF-II) receptor, which binds a variety of extracellular ligands, including the mammary mitogen IGF-II, and mediates their endocytosis and degradation (14). In contrast, this receptor also participates in the activation of the secreted latent TGFβ (15). *In vivo*, the anticancer effects of monoterpenes on liver, colon and mammary tumorigenesis are associated with inhibition of cellular proliferation and induction of apoptosis in regressing tumors (9,10,13,16,17). *In vitro*, limonene and perillyl alcohol inhibit cell proliferation (10) and induce apoptosis (K.Kim and M.N.Gould, unpublished data) in a variety of cell lines at doses within a pharmacologically achievable range. In this study, we focus on mechanisms underlying the cytostatic effect induced by monoterpene perillyl alcohol (POH) in the transformed murine mammary epithelial TM6 culture model.

Progression through the cell cycle is governed by a family of serine/threonine protein kinase complexes, which are composed of both a regulatory subunit (the cyclin) and a catalytic subunit (the cyclin-dependent kinase or Cdk) (18). The oscillation of specific Cdk activities dictates the temporal order of cell-cycle events. For example, one of the important molecular events required for passage through a rate-limiting G_1 phase preceding DNA synthesis, or the restriction point, is the inactivation of the retinoblastoma susceptibility gene product pRB by hyperphosphorylation by Cdks (19). pRB phosphorylation prevents pRB from binding with and regulating E2F transcription factors and thus allows the expression of E2F-responsive genes necessary for DNA replication and cell-cycle progression (20,21).

The activation of Cdks is regulated by various mechanisms including protein–protein interactions (with cyclins, Cdk inhibitors and assembly factors), protein degradation, transcriptional control, subcellular localization and multiple phosphorylation (22,23). D-type cyclins are induced as part of the delayed early responses to mitogenic stimuli. They form active holoenzymes with their catalytic partners Cdk4 and Cdk6 by mid-G_1, and are required for the initiation of G_1–S phase (19,24). Cyclin D-associated Cdks are responsible for the initial phosphorylation of pRB family proteins (18). Expression of cyclin E and the onset of its associated Cdk2 kinase activities is delayed relative to D-type cyclins, and is also rate-limiting for the G_1–S progression of the cell cycle (18). The cyclin E- and cyclin A-associated Cdk2 complete and/or maintain phosphorylation of pRB (18). One group of important negative

Abbreviations: POH, monoterpene perillyl alcohol; TGFβ, transforming growth factor β; Thr-160, threonine-160.

© Oxford University Press

regulators for Cdks are the Cdk inhibitors (CKIs), which fall into two distinct families based on their sequence homology. One family of CKIs includes $p16^{INK4a}$, $p15^{INK4b}$, $p18^{INK4c}$ and $p19^{INK4d}$. They act specifically on cyclin D–Cdk4/6 complexes by preventing cyclin D from binding (23,25). The second family of Cdk inhibitors includes $p21^{WAF1}$, $p27^{Kip1}$ and $p57^{Kip2}$. They were thought to be potent inhibitors of a wide range of cyclin–Cdk complexes (23,25). However, recent data suggest that Cip/Kip family inhibitors selectively inhibit cyclin–Cdk2 activities and are required for the activation for the cyclin D–Cdk4/6 *in vivo* (26–28). p21 is known to accumulate in response to DNA damage in a p53-dependent manner and can be induced in a p53-independent fashion (23).

Furthermore, the activities of Cdks can be both negatively or positively regulated by phosphorylation of critical residues in Cdks (22,29). Phosphorylation of a highly conserved threonine (Thr)-160 residue by a Cdk-activating kinase (CAK) is required for the Cdk activity (22). Interestingly, $p21^{WAF1}$ or $p27^{Kip1}$ in the Cip family or $p18^{INK4c}$ in the INK4 family can prevent CAK from phosphorylating the Cdk subunit by making the Thr-160-like site inaccessible to the CAK enzyme (30,31).

In this study, we have chosen the murine mammary epithelial TM6 cells as a model to study the effect of POH on cell proliferation and cell-cycle progression. We have found that POH treatment inhibited TM6 proliferation in a dose-dependent manner and caused cell-cycle arrest in the early G_1 phase and slowed the cell-cycle progression at the G_2–M phase. The early G_1 arrest was associated with the reduction in both cyclin D1-associated and cyclin E-associated kinase activities. POH treatment led to a reduction of cyclin D1 levels in asynchronous cells and prevented the formation of active cyclin D1-associated kinase complexes in synchronous cells during the exit of G_0. The reduction of cyclin E-associated kinase activity is consistent with an increased p21 association with cyclin E-associated kinase and a reduction of the activating phosphorylation of Cdk2 at the Thr-160 site.

Materials and methods

Reagents

(s)-(–)-Perillyl alcohol (>96% pure) was purchased from Aldrich (Milwaukee, WI). The following antibodies for western blot detection were used: monoclonal antibodies against cyclin D1 (72-13G and HD11), polyclonal antibodies against cyclin D1 (H-295), cyclin A (C-19), cyclin E (M-20), Cdk2 (M2), Cdk4 (C-22), Cdk6 (C-21) and pRB (C-15) from Santa Cruz Biotechnology (Santa Cruz, CA); monoclonal antibody against p21 (SXM30) and polyclonal antibody against p21 from PharMingen (San Diego, CA). All other materials were purchased from Sigma (St Louis, MO) if not otherwise indicated.

Cell culture

The murine transformed mammary epithelial TM6 cell line (32,33) was a generous gift from Dr Daniel Medina (Baylor College of Medicine, Houston, TX). Cells were maintained in Dulbecco's modified Eagle medium (DMEM)/Ham's F12 (1:1) medium (Sigma), pH 7.5, supplemented with HEPES buffer, heat-inactivated bovine serum (2%, HyClone Laboratories, Logan, UT), insulin (10 μg/ml, Collaborative Biomedical Products, Bedford, MA), epidermal growth factor (5 ng/ml, EGF, Collaborative Biomedical Products) and gentamycin (5 μg/ml, Gibco BRL, Gaithersburg, MD) at 37°C in 95% humidified air and 5% CO_2. The cells were routinely passaged using 0.1% trypsin–EDTA. To achieve synchronization at the G_0 phase of the cell cycle, TM6 cells were serum- and growth factor-starved for 48 h prior to the replacement with complete medium. To achieve a late G_1–early S phase synchronization, TM6 cells were treated with 200 mM mimosine (Sigma, stock solution prepared in 1 M NH_4OH) for 16 h, then washed and fed with complete medium.

Proliferation assay

One day before treatment, TM6 cells were plated into 6 well (35 mm diameter) culture plates in triplicate. Cells were either untreated or treated with various concentrations of POH. The cells were trypsinized and collected at the start of treatment (0 h), 9 and 19.5 h afterwards. The viable cells determined by trypan blue (Gibco BRL) exclusion were counted using a hemacytometer.

Cell-cycle analysis

TM6 cells were labeled with 20 mM bromodeoxyuridine (BrdU; Sigma) for 20 min, then trypsinized, harvested and fixed in 70% ethanol–0.34% Tween-20 at 4°C for at least 1 h. After digestion with pepsin, the resultant nuclei were incubated with a mouse anti-BrdU antibody (Becton Dickinson, San Jose, CA), followed by a fluorescein isothiocyanate (FITC)-conjugated goat anti-mouse secondary antibody (Sigma). The nuclear DNA was then stained with propidium iodide (PI; Boehringer Mannheim, Indianapolis, IN) overnight. Both DNA content and BrdU incorporation data were acquired and analyzed on a FACScan flow cytometry system (Becton Dickinson). Cell-cycle distribution was analyzed using ModFit LT 2.0 (Verity Software House, Topsham, ME) or CellQuest (Becton Dickinson Immunocytometry Systems, San Jose, CA) software. In all cases, proper gating was used to exclude doublets and other cell aggregates for analysis.

To follow cell-cycle progression through the S and G_2–M phases, actively proliferating TM6 cells were pulse-labeled with 1 mM BrdU (Sigma) for 30 min, and then the medium was replaced by fresh medium either with or without 0.5 mM POH. The cells were recovered at the start of treatment (0 h), 2, 5, 10 and 15 h afterwards, and flow cytometric assays were performed (20 000 events/determination). The BrdU-positive cells were gated for DNA content analysis using CellQuest software (Becton Dickinson).

Western blot analysis

Cell monolayers were washed twice with ice-cold phosphate-buffered saline (PBS) and cells were then scraped into ice-cold PBS and pelleted by centrifugation. The cell pellets were stored at –80°C before analyses. Cell lysates were prepared in ice-cold lysis buffer [50 mM HEPES, pH 7.5, 150 mM NaCl, 1 mM EDTA, 2.5 mM EGTA, 10% glycerol, 1 mM dithiothreitol (DTT), 0.1% Tween-20, 10 mM β-glycerophosphate, 1 mM NaF, 0.1 mM sodium orthovanadate, 0.1 mM PMSF, 1 mg/ml aprotinin, 20 mM leupeptin] followed by sonication 20 s in an ice-bath. The lysates were then clarified by centrifugation at 10 000 *g* for 15 min, and protein concentrations were determined by the bicinchonine acid (BCA) protein assay kit (Pierce, Rockford, IL). Thirty micrograms of protein per lane were resolved on either 12 or 15% SDS–PAGE gels for most analyses, or on 7.5% SDS–PAGE gels for pRB phosphorylation, and then transferred to 0.45 mm PVDF filter membranes (Millipore Corporation, Bedford, MA). The membranes were incubated with a specific antibody followed by a second antibody (anti-mouse IgG or anti-rabbit IgG) conjugated with alkaline phosphatase (Sigma) and proteins of interest were visualized using the Vistra Fluorescence Western blotting system (Amersham Life Science, Arlington Heights, IL) and a FluorImager (Molecular Dynamics, Sunnyvale, CA). Protein abundance was quantified using ImageQuant Software (Molecular Dynamics). The data displayed are representative of three or more independent experiments.

In vitro immune complex kinase assay and immunoprecipitation

The cell lysates were prepared as described as above. Equivalent amounts of protein were pre-cleared by incubating with normal serum and protein A/G–agarose (Cytosignal, San Diego, CA or Santa Cruz Biotechnology). For analysis of cyclin D1- or cyclin E-associated kinase activity, the kinase complexes were immunoprecipitated with 10 μl of mouse monoclonal anti-cyclin D1 (72-13G, Santa Cruz Biotechnology) or rabbit polyclonal anti-cyclin E (M-20, Santa Cruz Biotechnology) antibody, respectively, for 4 h followed by incubation with 20 μl of protein A/G–agarose (CytoSignal) for an additional 2 h. Immunoprecipitates were recovered by centrifugation, washed twice with lysis buffer, three times with base buffer (50 mM HEPES, pH 8.0, 10 mM $MgCl_2$ and 1 mM DTT), and once with kinase buffer (50 mM HEPES, pH 8.0, 10 mM $MgCl_2$, 2.5 mM EGTA, 1 mM DTT, 20 μmM ATP, 10 μM β-glycerophosphate, 0.1 mM sodium orthovanadate, 1 mM NaF). The kinase reaction was carried out at 30°C for 30 min by resuspending the beads in 40 μl of kinase buffer containing 10 mCi [γ-^{32}P]ATP (Dupont NEN) and 0.8 μg glutathione *S*-transferase (GST)–C-terminal pRB (QED Bioscience, San Diego, CA) to determine cyclin D1-associated kinase activity (250 μg protein/reaction), or that containing 2 μg histone H1 (Sigma) and 2 mCi [γ-^{32}P]ATP to determine cyclin E-associated kinase activity (100 μg protein/reaction) before it was terminated by addition of 5× SDS Laemmli's sample buffer. Unlabelled ATP (1 μl of 10 mM stock solution) was also added to each kinase reaction mixture following termination to reduce background. The reaction mixture was boiled for 5 min and resolved on 10% SDS–PAGE gels, which were later dried. Incorporation of ^{32}P into GST–pRB or histone H1 was quantitated using a PhosphorImager with ImageQuant software (Molecular Dynamics). The data displayed are representative of three independent experiments.

For examining the physical protein–protein interaction, the above pre-cleared cell lysates were adjusted by adding Nonidet-40 lysis buffer [50 mM

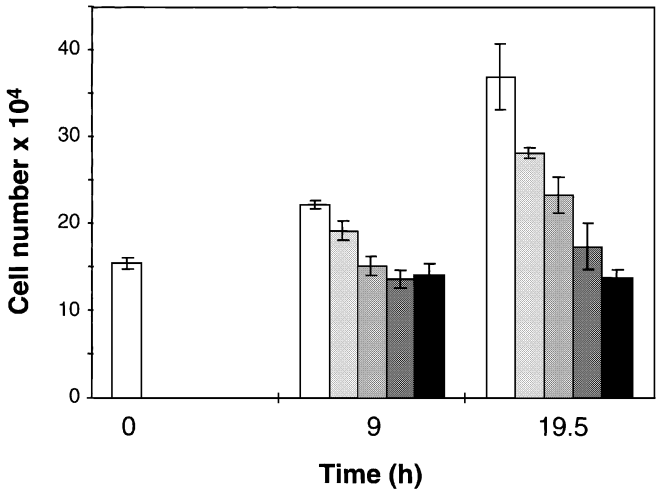

Fig. 1. Dose-dependent inhibition of TM6 cell proliferation by POH. Actively proliferating TM6 cells were plated into 6-well cell culture plates one day prior to POH treatment. The cells were then treated with various concentrations of POH. The viable cells (trypan blue excluding) were counted at the start of treatment (0 h) and 9 and 19.5 h post-treatment. Each data point in the plot represents the average number of viable cells per well from three wells. Each error bar denotes one standard deviation (SD) of the mean. Open bars, control; first right of open bar, cells treated with 0.1 mM POH; second right of open bar, cells treated with 0.3 mM POH; third right of open bar, cells treated with 0.5 mM POH; and fourth right of open bar, cells treated with 1 mM POH.

Tris–HCl, pH 7.5, 150 mM NaCl, 0.5% Nonidet-40, 50 mM NaF, 1 mM DTT, 1 mM Na_3VO_4, 1 mM phenylmethylsulfonyl fluoride (PMSF), 25 μg/ml leupeptin, 25 μg/ml aprotinin and 10 μg/ml trypsin inhibitor] as described by Jenkins and Xiong (34). The proteins of interest were immunoprecipitated with 10 μl of a specific antibody for 4 h followed by incubation with 20 μl of protein A/G–agarose (Santa Cruz biotechnology, or CytoSignal) for an additional 2 h. The agarose beads were recovered by centrifugation, and washed four times with Nonidet P-40 lysis buffer. After the final aspiration of lysis buffer, equal volume of 2× SDS Laemmli's sample buffer was added to the agarose and the precipitated proteins were denatured by boiling for 3 min, and separated in a 15% SDS–PAGE gel. The proteins of interest were detected by western blot analysis as described above.

Northern blot analysis

Total cellular RNA was extracted using RNeasy Mini kit (Qiagen, Chatsworth, CA). Ten micrograms of total RNA per lane were separated by formaldehyde–1% agarose gel electrophoresis, transferred to Zeta-Probe® nylon blotting membranes (Bio-Rad, Hercules, CA) using PosiBlot® Pressure Blotter (Stratagene, La Jolla, CA), and crosslinked using UV Stratalinker 2400 (Stratagene). A DNA probe used for murine *p21* mRNA detection was generated by PCR (1 min at 94°C, 1 min at 55°C, 1 min at 72°C) from cDNAs synthesized from mRNA isolated from murine Neuro-2A cells using SuperScript cDNA synthesis kit (Gibco BRL) using the primer pair: 5′-CACAGCGATATCCAGACATTC-3′ and 5′-CCTCCTGACCCACAGC-3′. Human cyclin-D1 cDNA was kindly provided by Dr David Boothman (Case Western Reserve University, Cleveland, OH). All DNA probes were labeled with [α-^{32}P]dATP or [α-^{32}P]dCTP using DECAprime II kit (Ambion, Austin, TX) and unincorporated nucleotides were removed by NICK® columns (Pharmacia, Piscataway, NJ). The hybridization was performed using QuickHyb (Clontech, Palo Alto, CA). Bands of interest were analyzed using a PhosphorImager with ImageQuant software (Molecular Dynamics). Equivalent loading of RNA samples was confirmed by hybridization with a DNA probe complementary to ribosomal 36B4.

Results

POH inhibits mammary epithelial TM6-cell proliferation

Actively proliferating TM6 cells were treated with various concentrations of POH and viable cells were then quantified over a period of 20 h. POH was able to inhibit TM6-cell proliferation in a dose-dependent manner. At doses of 0.5 mM and above, cell proliferation was blocked (Figure 1). Apoptosis, also quantified after 20 h exposure to 0.5 mM POH, which was minimal and comparable with the basal level (W.Shi, and M.N.Gould, data not shown). Therefore, the inhibition of cell proliferation by POH treatment in this cell line was not due to increased apoptosis but inhibition of proliferation.

POH treatment arrests TM6 cells in both the G_1 and G_2–M phases of the cell cycle

To determine if the POH-induced inhibition of cell growth involved specific cell-cycle arrest, cell-cycle distributions of exponentially growing TM6 cells treated with or without 0.5 mM POH were monitored by flow cytometric analysis. After 5 h of treatment, a modest increase in the G_2–M phase (18 ± 1% versus 11 ± 2% control) and a reduction in S phase (37 ± 3% versus 46 ± 3% control) were observed, whereas there was no difference in the percentage of G_1 phase cells at this point (Figure 2A). After 15 h, the percentage of cells in the G_1 phase increased to 63 ± 4% under POH treatment, the cells in the S phase decreased to 6 ± 1% (versus 40 ± 10% control), and the cells in the G_2–M phase increased to 22 ± 3% (versus 14 ± 4% control, Figure 2A).

We followed up the cell-cycle progression through the S and G_2–M phases in the BrdU pulse-labeled cells (Figure 2B). Cells, which were actively synthesizing DNA during a BrdU pulse of 30 min, were labeled. The majority of these BrdU-labeled cells entered the G_2–M phase within 5 h, subsequently exited from the G_2–M phase, and progressed into the G_0–G_1 phase in 10 h. The cells under POH treatment were slowed in their traversal of the G_2–M phase despite progressing through the S phase at similar rate as the untreated and were later arrested in the G_0–G_1 phase. Thus, POH exposure caused altered traversal at two points during the cell cycle, the G_0–G_1 phase and the G_2–M phase, while POH did not affect S phase progression. The arrest in the G_2–M phase induced by POH was transient when compared with the arrest in the G_1 phase.

Effects of POH on cell-cycle progression in synchronous TM6 cells

We next focused on examining the effects of POH on the G_1–S progression of cells synchronized either by release from quiescence (G_0) or from late G_1. TM6 cells were synchronized in G_0 phase by serum and growth factor starvation for 48 h and followed by re-feeding with complete growth medium. Cell-cycle progression after release from serum starvation was evaluated by flow cytometric analysis for both BrdU incorporation and DNA content (Figure 2C). Between 70 and 80% of the cells were arrested in the G_0 phase after serum starvation for 48 h. Ten hours after release by serum addition, 30% of TM6 cells progressed into early S phase. After 15 h, 60% of cells entered the S phase, while after 21 h the majority of cells passed through the G_2–M phase and entered the subsequent G_1 phase. In contrast, the majority (65–80%) of cells exposed to 0.5 mM POH concurrently with serum addition remained in the G_0–G_1 phase.

We then examined the cell-cycle progression in TM6 cells synchronized by the plant non-protein amino acid mimosine. Mimosine has been shown to reversibly arrest cells in the late G_1 or early S phase (35–37). The cells were synchronized by release from mimosine incubation. Cell-cycle progression in the presence of or absence of POH was evaluated by flow cytometric analysis of BrdU incorporation and DNA content. After release from the mimosine block, both untreated cells and cells treated with POH entered the early S phase in ~2 h

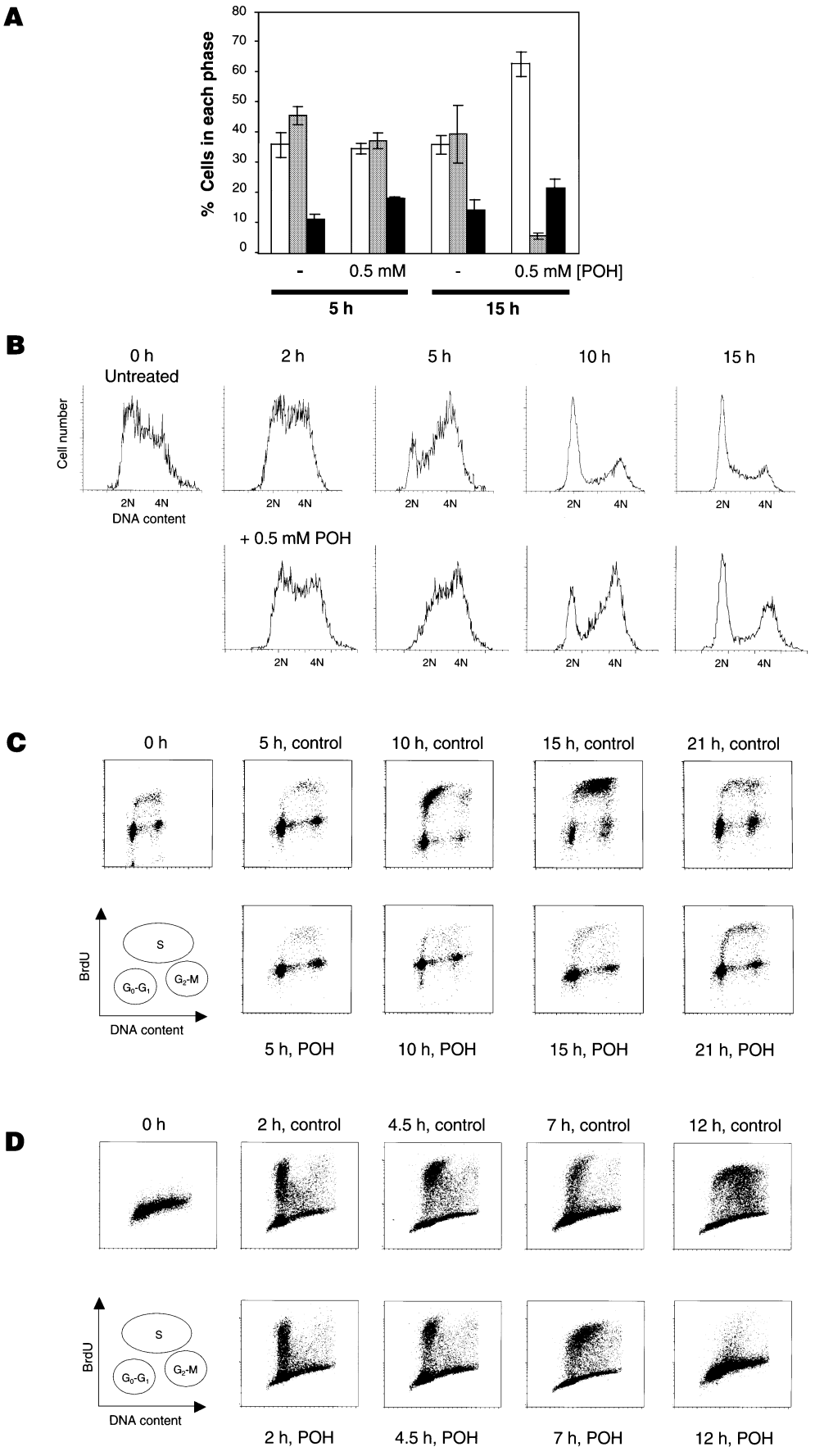
A
% Cells in each phase
80
70
60
50
40
30
20
10
0
-
0.5 mM
-
0.5 mM [POH]
5 h
15 h
B
0 h
Untreated
2 h
5 h
10 h
15 h
Cell number
2N
4N
DNA content
+ 0.5 mM POH
C
0 h
5 h, control
10 h, control
15 h, control
21 h, control
BrdU
S
G0-G1
G2-M
DNA content
5 h, POH
10 h, POH
15 h, POH
21 h, POH
D
0 h
2 h, control
4.5 h, control
7 h, control
12 h, control
2 h, POH
4.5 h, POH
7 h, POH
12 h, POH

(Figure 2D). Within 4.5 h, similar percentages of cells entered the S phase. POH treatment did not prevent the onset of S phase and the S to G_2–M cell-cycle progression up to this point. Twelve hours after release, the control cells completed mitosis and progressed through the S phase, while the cells treated with POH were blocked at the G_2–M phase and/or the subsequent G_0–G_1 phase. Thus, the G_1 cell-cycle blockage point of POH appears to be located at early G_1 to mid-G_1. Once the cells pass into the late G_1, the completion of S phase seems to be less sensitive to POH treatment.

Inhibition of pRB phosphorylation and cyclin D1- and cyclin E-associated Cdk activities by POH treatment in asynchronous cells

As pRB phosphorylation has been associated with the G_1–S transition, we investigated the phosphorylation status of pRB in response to POH treatment in asynchronous cells. Phosphorylated pRB is indicated by a retarded electrophoretic mobility in denaturing polyacrylamide gels in comparison to unphosphorylated or hypophosphorylated pRB. In asynchronously growing TM6 cells, the majority of pRB was hyperphosphorylated (the slower migrating forms). In contrast, in cells exposed to 0.5 mM POH for 5 and 15 h, the percentage of cells in the G_1, S, G_2–M phases were 62.9, 6.0 and 15.6% for the POH-treated cells versus 36.1, 39.5 and 14.4%, respectively, for the untreated cells. The hyperphosphorylated pRB forms (slower migrating) were reduced, as the hypophosphorylated forms (faster migrating) increased (Figure 3A). Therefore, POH treatment resulted in the inhibition of pRB phosphorylation.

The activities of G_1 Cdks, cyclin D1-associated and cyclin E-associated kinases, which have been shown responsible for the phosphorylation of pRB during the G_1–S transition (18), were then examined. After 5 h, there was no significant difference in the cyclin D1-associated kinase activities (106% of the untreated, $P = 0.729$, $n = 3$) in the POH-treated cells between the untreated cells (Figure 3B) or cyclin E-associated kinase activities in the POH treated cells (80.9% of the untreated, $n = 3$, $P = 0.116$, Figure 3C). However, after 15 h, the cyclin D1-associated kinase activities were inhibited by 33.8% ($n = 3$, $P = 0.041$, Figure 3B) and the cyclin E-associated kinase activity was dramatically reduced by 85.8% ($n = 3$, $P = 0.001$, Figure 3C).

Effects of POH on levels of cyclins Cdks, and the Cdk inhibitor $p21^{WAF1}$ in asynchronous cells

To address how the cyclin-associated kinase activities are affected by POH treatment, we examined the expression of cyclins and Cdks involving the G_1–S transition in asynchronous TM6 cells. POH treatment reduced the cyclin D1 protein levels by 14% ($P = 0.053$, $n = 3$) after 5 h and by 47% ($P = 0.017$, $n = 3$) after 15 h, respectively (Figure 4A). Such a reduction in cyclin D1 protein levels might be responsible for the reduction in the cyclin D1-associated kinase activity after 15 h (Figure 3B). Meanwhile, no difference in the levels of cyclin E and Cdk4 proteins were observed in these cells (Figure 4B), whereas cyclin A protein levels were slightly but reproducibly reduced, followed by a reduction of the percentage of cells in the S phase after 15 h treatment of POH (Figure 4B).

To address how POH treatment resulted in an inhibition of the cyclin E–Cdk2 activities, we then examined the Cdk inhibitor $p21^{WAF1}$. POH treatment caused an increase of *p21* message levels in a dose-dependent manner within 5 h (Figure 4C). The total cellular p21 levels were modestly increased under POH treatment (Figure 4D). In addition, the association of $p21^{WAF1}$ with cyclin E–Cdk2 complex was determined by western blot detection of $p21^{WAF1}$ in the cyclin E–Cdk2 complexes immunoprecipitated with an anti-cyclin E antibody. Cyclin E complexes from actively proliferating cells were generally free of p21. Within 5 h, POH treatment caused a dramatic increase (2–3-fold) in the amounts of p21 in the cyclin E–Cdk2 complexes, whereas similar amounts of Cdk2 were present in the complexes. The increased p21 association with cyclin E–Cdk2 complexes was maintained at 15 h (Figure 4D). In contrast, the association of p21 with cyclin D1–Cdk complexes was not affected by POH treatment (Figure 4D).

We also examined the effect of POH treatment on the phosphorylation of Cdk2 at Thr-160 site, which is required for the full activation of Cdk2 (22). The detection of the Thr-160 phosphorylated Cdk2 benefited from its faster electrophoretic mobility on denaturing polyacrylamide gels compared with that of the unphosphorylated form (38). In asynchronous TM6 cells, POH treatment for 15 h caused a decrease in the abundance of the faster migrating form of Cdk2, which represents the active Thr-160 phosphorylated form (Figure 4E). Such a decrease of the active form of Cdk2 occurs later compared with the increased binding of $p21^{WAF1/Cip1}$ with cyclin E–Cdk2 complexes (Figure 4D) and correlated well with the reduction of cyclin E–Cdk2 kinase activity (Figure 3C).

Inhibition of pRB phosphorylation and G_1 Cdk activities by POH treatment in synchronous cells

We also followed up the changes induced by POH treatment in synchronous TM6 cells released from serum starvation. In cells under serum and growth factor starvation (in the G_0 phase), the majority of pRB was unphosphorylated (the faster migrating band, Figure 5A). Starting from 5 h after release from the serum starvation, the pRB became phosphorylated

Fig. 2. The POH-induced G_1 and G_2–M cell-cycle arrest. (**A**) Asynchronously growing TM6 cells were either untreated or treated with 0.5 mM POH for 5 or 15 h. Cell-cycle distributions were analyzed by flow cytometric analysis of DNA content and the S phase distributions were determined by BrdU incorporation using 10 000 cells/determination with CellQuest software. Open bars represent the percentages of cells in the G_0–G_1 phase, speckled bars represent the percentages of cells in the S phase, and solid bars represent the percentages of cells in the G_2–M phase. (**B**) Effect of POH treatment on cell-cycle progression through the S and G_2–M phases. Asynchronous TM6 cells were labeled with 1 mM BrdU for 30 min, and then the medium was replaced with medium without BrdU. The cells were either untreated or treated with 0.5 mM POH. The cells were collected at the start of treatment (0 h) and 2, 5, 10 and 15 h afterward. Cell-cycle distributions of the BrdU-positive cells are displayed in histograms of DNA content after flow cytometric analysis. (**C**) The blockage of the G_1–S transition by POH in synchronous cells released from G_0. TM6 cells were synchronized by release from serum and growth factor deprivation for 48 h and were either untreated or were treated with 0.5 mM POH immediately after release from serum starvation (0 h). The cells were collected at various time points as indicated above. The cell-cycle distributions are displayed after flow cytometric analysis of DNA content and BrdU incorporation using 10 000 cells/determination with CellQuest software and presented in dot plots of BrdU fluorescence (*y* axis) versus DNA content (*x* axis). (**D**) Inability of POH to block cell-cycle progression following release from a late G_1/early S block. TM6 cells were arrested at a late G_1/early S phase by 200 μM mimosine for 16 h. The cells were either untreated or treated with 1 mM POH immediately after release from mimosine treatment and collected at various time points as indicated above. Cell-cycle distributions were presented here in dot plots of BrdU fluorescence (*y* axis) versus DNA content (*x* axis) after flow cytometric analysis (20 000 cells/determination).

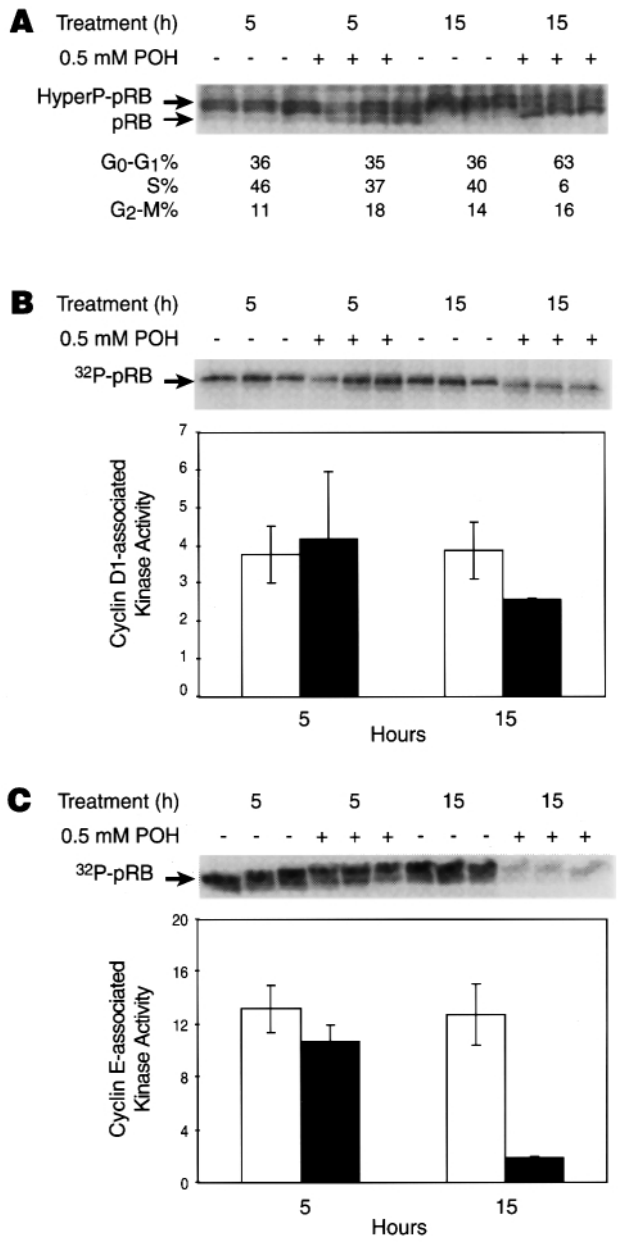

Fig. 3. Inhibition of pRB phosphorylation and of the G_1–S cyclin-dependent kinase activities by POH treatment in asynchronous cells. Actively cycling TM6 cells were either untreated (–) or treated with 0.5 mM POH (+) for 5 or 15 h and total cell lysates were then prepared. Cell-cycle distributions in parallel cell cultures were determined by flow cytometric analysis of DNA content. (**A**) Lysates containing 30 mg of protein were resolved on a 6.5% SDS–PAGE gel and pRB protein was detected by western blot analysis. (**B**) Cyclin D1- or (**C**) cyclin E-associated kinase activities in lysates were assayed and quantified. The open bars in the histograms represent kinase activities in lysates from control cells and solid bars represent those in lysates from POH-treated cells. The data displayed are the averages from three experiments. Each error bar denotes 1 SD of the mean.

(the slower migrating forms) as the cells underwent the G_1 to S transition and entered the S phase subsequently. However, pRB in cells under POH remained as the slower migrating forms, presumably unphosphorylated or hypophosphorylated, as the cells were arrested at the G_0–G_1 phase during the period of POH treatment.

The cyclin D1-associated kinase activities in the cell lysates were determined by immune complex kinase assays. Five hours post-release, the cyclin D1-associated kinase activities were slightly increased in both control and POH-treated cells (Figure 5B). Ten hours post-release, the cyclin D1-associated kinase activity in the untreated cells peaked, which correlated to cell entry into the early S phase (~30% S phase). However, POH treatment effectively blocked such an induction of cyclin D1-associated Cdk activities at 10 h ($P = 0.03$, $n = 3$); the treated cells remained in the G_0–G_1 phase as indicated by a lack of S phase progression. Cyclin E-associated kinase activities in cell lysates were also assayed (Figure 5C). In the untreated cells, the cyclin E-associated kinase activities were greatly induced 10 and 15 h after released from serum deprivation. The peak kinase activity after 15 h correlated to the onset of S phase (60%). In contrast, no induction of cyclin E-associated kinase activities was observed in cells under POH (at 10 h, $P = 0.004$; at 15 h, $P = 0.01$, Figure 5C) as the cells were arrested at the G_0–G_1 phase of the cell cycle.

Effects on the levels of cyclins, Cdks, p21 and the Cdk2 phosphorylation by POH treatment in synchronous cells

To understand how cyclin D1-associated kinase activities were affected by POH treatment in the synchronous cells, we examined the cyclin D1 protein levels. As predicted, cyclin D1 protein levels increased as cells exited quiescence and progressed through the G_1 and S phase. Whereas over 70% cells did not progress through the G_1 phase under POH treatment, surprisingly similar levels of cyclin D1 were present in the untreated and the 0.5 mM POH-treated cells (Figure 6A) despite an attenuated induction of *cyclin D1* mRNA levels (Figure 6C) and lack of cyclin D1-associated kinase activities in the POH-treated cells (Figure 5B). Only POH at a dose of 1 mM blocked the induction of cyclin D1 protein totally along with the induction of the cyclin D1-associated kinase activity (data not shown). POH treatment did not change the protein levels of Cdk4 either (Figure 6A). Furthermore, when the association of Cdk4 and cyclin D1 was examined by western blot analysis in cyclin D1 immunoprecipitate, comparable levels of D1 were associated with Cdk4 in the POH-treated cells and in the untreated cells (Figure 6A). Similar levels of Cdk6 were associated with cyclin D1 in the untreated and in the POH-treated cells (Figure 6B). The results suggest that some as yet unknown mechanisms, other than prevention of cyclin D1 and Cdk4/6 interaction but still forming functional cyclin D1–Cdk4/6 complexes, were responsible for the POH inhibition of cyclin D1-associated kinase activities during the exit of G_0.

We also examined how the cyclin E-associated kinase activities were affected by POH treatment. In POH-treated cells, the levels of various forms of cyclin E, which have been reported to be expressed in TM6 cells (39), were not different from the untreated cells (Figure 6A). A prominent induction of S phase expressing cyclin A was observed in control cells during cell-cycle progression into the S and the G_2–M phase. However, such an induction of cyclin A was prevented by treatment of 0.5 mM POH (Figure 6A), which is not surprising due to a lack of S phase entry under POH treatment.

In synchronized TM6 cells, the p21 message and protein levels increased as the cells exited quiescence (Figure 6C and D). The total cellular p21 protein levels in the POH-treated cells were modestly but consistently higher (by 10–30%) than those in the control cells (Figure 6D). Furthermore, the association of p21 with the cyclin E–Cdk2 complex was increased by 2- and 5-fold at 10 and 15 h, respectively, by POH treatment (Figure 6D) in contrast to the minimal p21

association with cyclin E in untreated cells. POH treatment further increased *p21* transcript levels compared with untreated cells (Figure 6C). Meanwhile, the levels of p21 associated with the cyclin D1–Cdk complexes were generally comparable in both the POH-treated cells and the control cells (Figure 6B). Therefore, the increase of p21 in cyclin E–Cdk2 complexes may also result from a specific interaction with in the cyclin E–Cdk2 complexes independently of the increase in total cellular p21 protein levels.

In addition, Cdk2 protein levels remained constant under 0.5 mM POH while increased 2-fold in the control (Figure 6A). Using 15% SDS–PAGE gel, the different phosphorylated forms of Cdk2 at Thr-160 site can be separated. The relative abundance of the active form of Cdk2 (faster migrating)

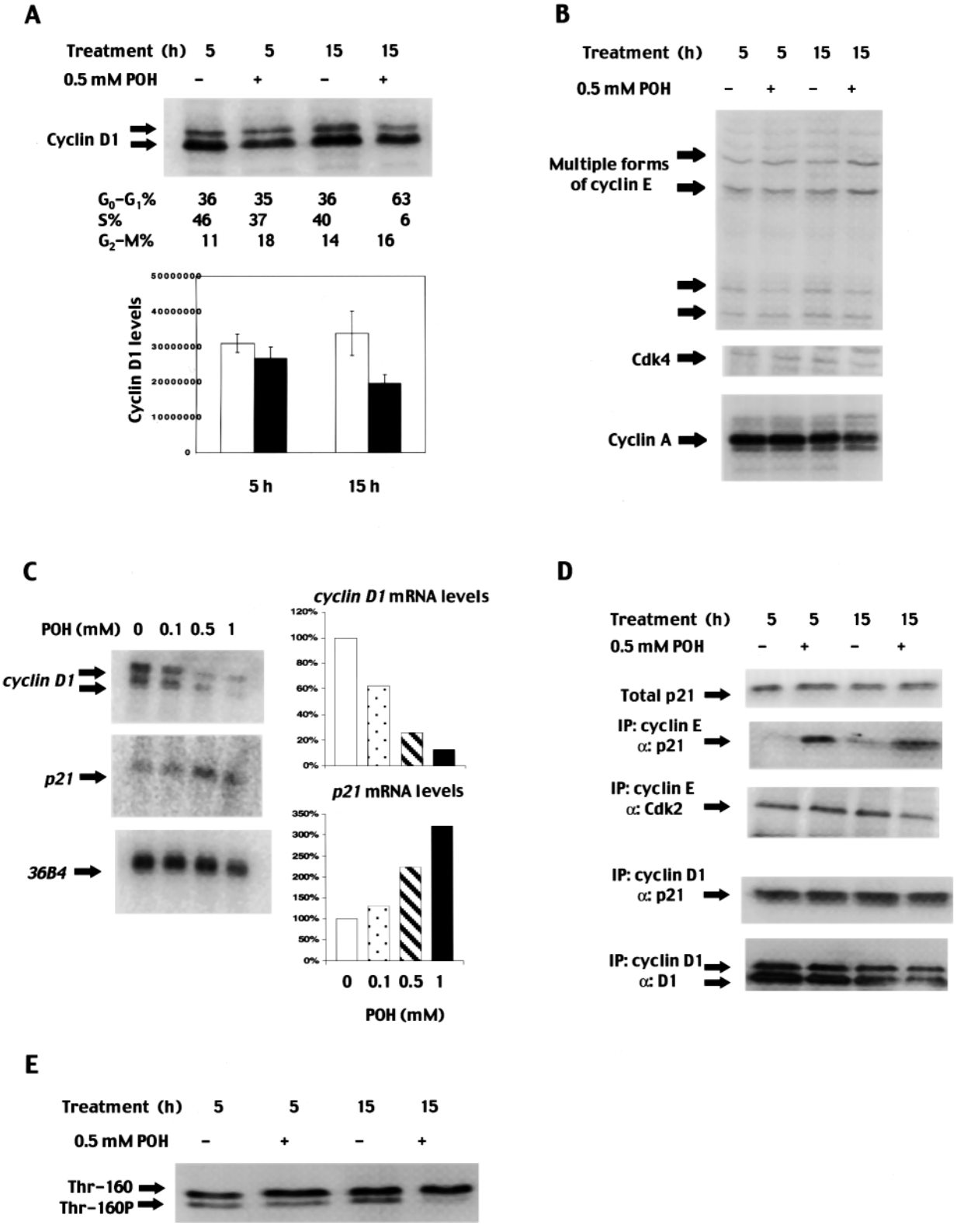

increased at 15 h as the untreated cells progress through the G_1 and S phase. Such an increase was modestly inhibited in the POH-treated cells (Figure 6E). A comparison of the effects of POH on cell-cycle related molecules is given in Table I.

Discussion

Monoterpenes have been shown to have anticancer activities for both cancer chemoprevention and chemotherapy in a wide variety of pre-clinical *in vitro* and *in vivo* cancer models. For example, POH can both treat and prevent rat mammary carcinomas. Monoterpene activities at the cellular level in rat mammary cancer treatment are associated with the inhibition of cancer-cell proliferation and the induction of apoptosis (13). *In vitro*, POH has been shown to inhibit cell proliferation and induce apoptosis in a wide variety of cell lines (10). It is thus likely that the cytostatic and apoptotic effects of POH might contribute to the anticancer activity of monoterpenes. In this study, we investigated mechanisms underlying the cytostatic effect of POH in a murine transformed mammary epithelial cell line TM6. POH treatment inhibited the cell proliferation and DNA synthesis in TM6 cells in a dose-dependent manner. The dose of 0.5 mM POH mainly in this study was chosen based on the similar non-toxic serum levels of monoterpenes in rats (40) and humans (4,5). In addition, the TM6 cell line showed little apoptosis ($<3\%$) as determined by TUNEL assay after exposure to 0.5 mM POH for up to 20 h, which allowed us to independently focus on the cytostatic effect of POH.

POH treatment affects the cell cycle by causing a G_1 arrest and a transient G_2–M arrest. Extended POH exposure results in an accumulation of cells predominantly in the G_1 phase (data not shown). Examination of the cell-cycle progression of the BrdU pulse-labeled cells further suggested that the G_2–M arrest caused by POH treatment is incomplete and transient. The underlying mechanism of the G_2–M arrest induced by POH has yet to be identified. POH treatment blocked the S-phase entry in synchronous cells released from serum starvation; however, it did not affect the S phase progression in cells pre-treated with and released from mimosine. Therefore, the POH-induced G_1 arrest occurs at early to mid-G_1. Such an arrest position appears to reside earlier than the late G_1 proximal to G_1–S border or at early S phase, the acting point of mimosine induced cell-cycle arrest (35).

We have thus focused on studying the molecular factors involved in the regulation of G_1–S transition, as they are less likely the consequence of cell-cycle arrest. In contrast, the expression of factors associated with other cell-cycle phases, such as the reduced expression of S phase cyclin A, may be due to lack of cell-cycle progression. To distinguish the molecular changes associated with the G_1 block and the cause of G_1 arrest, we have examined these changes in both asynchronous cells and synchronous cells released from serum starvation. We found that the early G_1 arrest may be in part related to the effect of POH treatment on pRB phosphorylation. In addition, POH treatment reduced cyclin D1-associated kinase activities. Furthermore, POH treatment induced an increase in the association of Cdk inhibitor p21 with cyclin E–Cdk2 complexes and inhibited the activating phosphorylation of Cdk2.

Among all changes associated with the G_1 arrest, we found that an increase of p21 association with cyclin E–Cdk2 complexes might be important in causing G_1 arrest. Such an increase of p21 binding with cyclin E–cdk2 complexes happens in asynchronous cells after 5 h exposure to POH, whereas there is no major change in cell-cycle distribution. The paradox is that at this 5 h timepoint we did not observe a major inhibition of the cyclin E-associated kinase activities. It is possible that the inhibition of cyclin E-associated kinase activity may also require an inhibition of activating phosphorylation of Cdk2 at Thr-160 site. Hitomi *et al*. has reported that elevated p21 association with cyclin E–Cdk2 induced by prostaglandin A2 could not completely account for the reduction in kinase activity and the activating phosphorylation of Cdk2 at the Thr-160 site which correlates most closely with the inhibition of kinase activities (41). However, here the reduction in active phosphorylation of Cdk2 appears later than the induction of $p21^{WAF1}$. Although we could not exclude the possibility that POH treatment might affect CAK, we suggest that POH treatment induced p21 association with cyclin E–Cdk2 complexes. However, the consequence of this interaction, the major inhibition of cyclin E-associated kinase activity, may occur later when the Cdk2-activating phosphorylation is inhibited as a result of a blockage of CAK from phosphorylating Cdk2 by p21.

The increased p21 association with cyclin E–Cdk2 complexes thus may have resulted partly from the increase in total cellular p21 protein levels and partly from a specific protein–protein interaction. In TM6 cells, POH exposure (at 0.5 mM) resulted in a 2-fold increase in the *p21* mRNA levels after 5 h treatment. The increase in *p21* mRNA levels caused by POH treatment may be due to increased *p21* gene transcription, as such an increase is sensitive to the RNA synthesis inhibitor actinomycin D (data not shown). *p21* was initially found under the transcriptional control of wild-type p53, especially following DNA damage (23). However, *p21* can also be induced by p53-independent mechanisms. In the TM6 cell

Fig. 4. Effects of POH treatment on cyclins, Cdks and p21 in asynchronous cells. Actively cycling TM6 cells were either untreated or treated with POH. Cell-cycle distributions in parallel cell cultures were determined by flow cytometric analysis of DNA content. The data displayed are representative of three independent experiments. (**A**) Total cyclin D1 protein in lysate each containing 30 mg of total cellular protein was detected by western blot analysis with an anti-cyclin D1 antibody. The levels of cyclin D1 were quantitated using ImageQuant software after visualization on a FluorImager. (**B**) The association of $p21^{WAF1}$ with cyclin D–Cdk complex was determined by immunoprecipitation of cyclin D1 with an anti-cyclin D1 antibody and followed by western blot analyses for Cdk6, cyclin D1 and $p21^{WAF1}$. (**C**) Dose-dependent effects of POH on *cyclin D1* and *p21* levels. Total RNA was extracted from actively growing TM6 cells either untreated (0) or treated with 0.1, 0.5 or 1 mM for 4.5 h. Northern blot was hybridized with ^{32}P-labeled DNA probes for *cyclin D1* and *p21*. The histogram presents representative *cyclin D1* and *p21* mRNA levels (in percentage of the control) quantitated with a PhosphorImager and ImageQuant software after being normalized to *36B4* ribosomal RNA for loading. The cyclin D1, Cdk2 and $p21^{WAF1}$ proteins were detected by western blot analyses after visualization on a FluorImager using ImageQuant software. Similar trends are observed in repeat experiments. (**D**) The association of $p21^{WAF1}$ with cyclin E–Cdk2 complex was determined by immunoprecipitation of cyclin E with an anti-cyclin E antibody and followed by western blot analysis for Cdk2 and $p21^{WAF1}$. The total cellular p21 protein in lysates containing 30 mg of total cellular protein was detected by western blot analysis. The association of $p21^{WAF1}$ with cyclin D–Cdk complex was determined by immunoprecipitation of cyclin D1 with an anti-cyclin D1 antibody and followed by western blot analyses for cyclin D1, and $p21^{WAF1}$. (**E**) The Thr-160 phosphorylated (the faster migrating band) and the unphosphorylated (the slower migrating band) Cdk2 were were resolved on a 15% SDS–PAGE gel and detected by western blot analysis.

line, both alleles of the *p53* gene are mutated with a Trp^{138} substitution and a D123–129 allele in *p53* gene (33). Therefore, the upregulation of *p21* mRNA by POH is independent of functional p53 protein. Based on our biochemical studies of these monoterpenes and findings by others on p21-inducing agents, we speculate a possible linkage of the POH-induced inhibition of protein isoprenylation with p21 induction. POH treatment inhibits the mevalonate pathway downstream of HMG-CoA reductase (8,10,11). This inhibition includes inhibiting geranylgeranyl protein transferase (GGPT) activity (42). Interestingly, the HMG-CoA reductase inhibitor lovastatin and specific GGPT inhibitors induces *p21* mRNA independent of p53 (43,44). Furthermore, the geranylgeranylated small G protein Rho has been linked to a repression of p21 upregulation in response to Raf activation (45,46). The induction of p21 by POH treatment is potentially mediated through the disruption of isoprenylated protein functions.

Compared with the POH-induced increase in the *p21* message RNA levels, the increase in total cellular p21 protein levels ranged from 0.5- to 2-fold in POH treated asynchronous cells and modestly increased by 10–30% in synchronous cells when compared with the control cells. Nevertheless, POH treatment caused a more dramatic increase in the association of p21 with cyclin E–Cdk2 complexes. In contrast, the association of p21 with cyclin D1–Cdk complexes did not increase. It is yet unclear how such a specific increase of p21 association with cyclin E complex was achieved by POH treatment. It has been proposed that an important function of D-type cyclins is acting to sequester p21 from binding with cyclin E complexes (25). It is possible that the reduction of D-type cyclins by POH treatment could lead to more p21 available for interacting with cyclin E complexes.

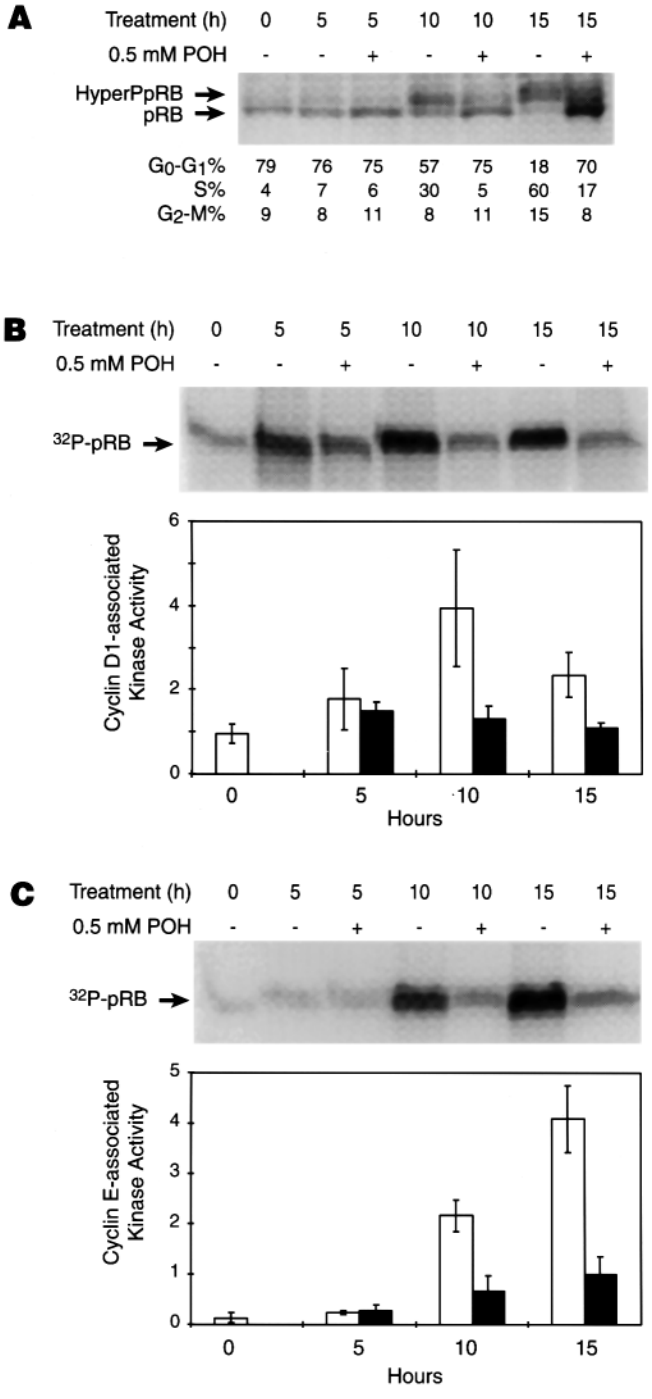

Table I. Effects induced by 0.5 mM perillyl alcohol in asynchronously growing and synchronously growing TM6 cells

	In asynchronously growing cells	In synchronously growing cells released from serum starvation
Percent of cells in G_1 phase	Up at 15 h	Remain high
pRB hyperphosphorylation	Down	Down
Cyclin D-associated kinase activity	Unchanged at 5 h, down at 15 h	Uninduced at 10 h
Cyclin D1 mRNA	Down at 5 h	Down at 5 h
Cyclin D1 protein	Unchanged at 5 h, down at 15 h	Unaffected
Cyclin D-associated Cdk4/6	Down at 15 h (data not shown)	Unaffected
Cyclin E-associated kinase activity	Down at 15 h	Uninduced at 10 h and 15 h
p21 mRNA	Up	Up
p21 protein	Up modestly at 5 and 15 h	Up modestly
Cyclin E–Cdk2-associated p21	Up at 5 and 15 h	Up at 10 and 15 h
Active Cdk2 protein	Down at 15 h	Down at 10 and 15 h
Cyclin A protein	Down at 15 h	Uninduced

Fig. 5. Inhibition of pRB phosphorylation and of the G_1–S cyclin-dependent kinase activities by POH treatment in synchronous cells. TM6 cells were synchronized by release from serum and growth factor deprivation. The cells were either untreated (–) or treated with 0.5 mM POH (+) starting at release from serum starvation and collected at various time points post-treatment. Total cell lysates were then prepared. Cell-cycle distributions in parallel cell cultures were determined by flow cytometric analysis of DNA content. (**A**) Lysates, each containing 30 mg of protein, were resolved on a 6.5% SDS–PAGE gel and pRB protein was detected by western blot analysis using an anti-pRB antibody. (**B**) Cyclin D1-associated kinases or (**C**) cyclin E-associated kinases in lysates were immunoprecipitated with an antibody specific for cyclin D1 or cyclin E, respectively. The kinase activities in the immune complexes were assayed (recombinant pRB used as a substrate for cyclin D1-associated kinase assay and histone H1 used as a substrate for cyclin E-associated kinase assay) and the reaction mixture was separated by denaturing polyacrylamide gel electrophoresis. The kinase activities (in arbitrary units) were the amount of ^{32}P incorporated into the substrate determined by a PhosphorImager and ImageQuant analysis. The open bars in the histograms represent kinase activities in lysates from control cells and solid bars represent those in lysates from POH-treated cells. The data displayed are the averages from three experiments. Each error bar denotes 1 SD of the mean.

In addition, in synchronous cells released from serum starvation (during the cell-cycle entry from quiescence), POH treatment prevented the induction of cyclin D1-associated kinase activity. In contrast, the inhibition of cyclin D1-associated kinase activities by POH treatment in asynchronous cells was less dramatic. This could be due to differences

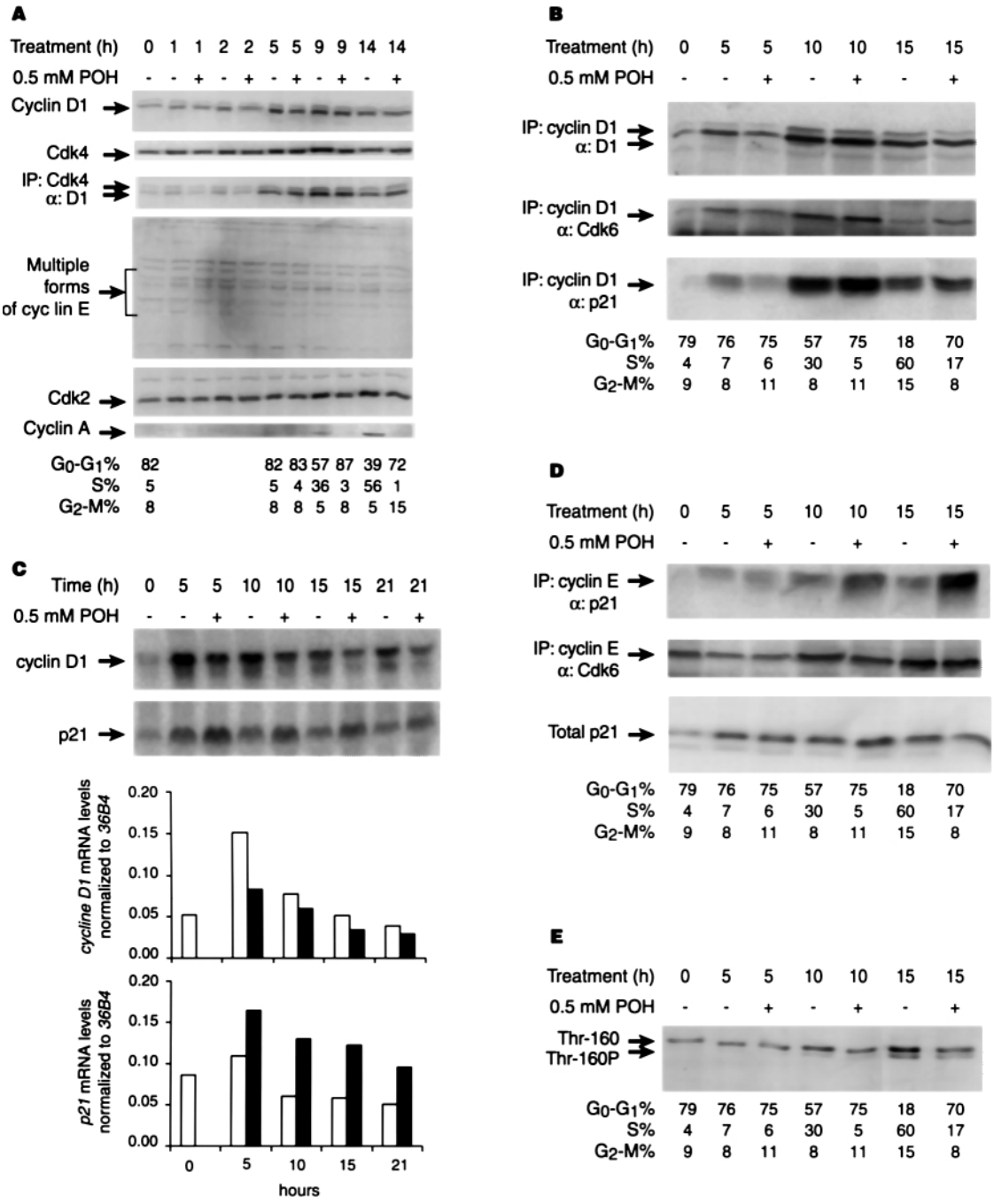

Fig. 6. Effect of POH on cyclins, p21 and Cdks expression in synchronous cells. Cells were recovered at various time points from untreated (–) or POH-treated (+) cells released from G_0 arrest by serum and growth factor deprivation. Cell-cycle distributions in parallel cell cultures were determined by flow cytometric analysis of DNA content. The data displayed are representative of three independent experiments. (**A**) Cyclin D1, Cdk4, cyclin E, Cdk2 and cyclin A in cell lysates containing 30 mg of total cellular protein were detected by western blot analyses. The complex formation of cyclin D1 and Cdk4 was determined by western blot detection of cyclin D1 coimmunoprecipitated with Cdk4. TM6 cells expressed multiple forms of cyclin E. (**B**) Complex formation of Cdk6 with cyclin D1 and association of p21 were examined by immunoprecipitation of cyclin D1 followed by western blot analysis for Cdk6 and p21, respectively. (**C**) Northern blot analysis of *cyclin D1* and *p21* mRNA levels. Total RNA was isolated from untreated (–) cells or cells treated with 0.5 mM POH (+) for the times indicated. *Cyclin D1* and *p21* mRNA were detected by northern blot analysis. The same blot was hybridized with a DNA probe for constitutively expressed *36B4* ribosomal RNA to normalize the loading of RNA per lane. The abundance of RNAs was quantitated with a PhosphorImager and ImageQuant software after being normalized to *36B4* ribosomal RNA and was plotted in arbitrary units. Open bars represent the control and solid bars represent the 0.5 mM POH-treated cells. (**D**) The association of $p21^{WAF1}$ with cyclin E–Cdk2 complex was determined by immunoprecipitation of cyclin E with an anti-cyclin E antibody and followed by western blot analysis for Cdk2 and $p21^{WAF1}$. The total cellular p21 protein in lysates containing 30 mg of total cellular protein was detected by western blot analysis. (**E**) Inhibition of the activating phosphorylation of Cdk2 by POH treatment. The faster migrating Cdk2 band (resolved on a 15% SDS–PAGE gel and detected by western blot analysis) represents the Cdk2 phosphorylated at Thr-160.

between cells that move from a quiescent state to a proliferative state and actively proliferating cells traversing G_1. As the former cells exit from the G_0 phase, cyclin D1 is synthesized in the cytoplasm, assembled with its kinase partners Cdk4 and Cdk6 into complexes, and translocated into the nuclei in response to serum-mediated signaling (47). POH treatment may block the induction of cyclin D1-associated kinases by preventing the synthesis or activation of unidentified rate-limiting activating regulator(s), which are responsible for the formation or proper localization of active cyclin D–Cdk complexes. In contrast, in actively cycling cells, the activating factor(s) for cyclin D–Cdk complexes are not rate-limiting. POH-induced inhibition of cyclin D1-associated kinase activity reflects the downregulation of cyclin D1 proteins.

Furthermore, surprisingly equivalent levels of cyclin D1–Cdk6 and cyclin D1–Cdk4 complexes exist in control and 0.5 mM POH-treated synchronized TM6 cells released from serum starvation despite the strong inhibition of cyclin D1-associated kinase activity caused by POH treatment. Therefore, some mechanisms other than those preventing cyclin D1–Cdk6 complex formation could be involved to inhibit cyclin D1–Cdk activities. Among a number of possibilities, it is unlikely due to currently known CKIs. The inhibitors of the INK4 family would disrupt the association of Cdk4/6 with cyclin D (23,25). In addition, the members of the Kip family, p21 and p27, were found to be associated with cyclin D1; however, their association may play activating roles in cyclin D–Cdk4/6 complex formation (25). In our case, no correlation between the p21 or p27 association and the inhibition of cyclin D–Cdk4/6 activity was found following POH treatment (Figures 4D, 6B and data not shown). Alternatively, POH treatment might affect the post-translational modifications of cyclin D1–Cdk4/6 complexes, such as the phosphorylation state of Cdk4 and Cdk6. For example, the tyrosine phosphorylation regulation of Cdk4 has been shown to be associated with the cell-cycle exit into the G_0 phase, contact inhibition (48), and G_1 arrest induced by UV irradiation and TGFβ treatment (49,50). Finally, POH treatment could prevent the formation of active cyclin D1–Cdk4/6 holoenzymes by affecting additional factors in cyclin D1–Cdk4/6 complexes and subcellular localization of the complexes. It has been shown by Mahony *et al*. that only the nuclear localized cyclin D–Cdk6 complexes with estimated molecular mass of 150–170 kDa are catalytically active in T cells (51). Similar complexes were also observed in mammary epithelial cells (52). The identity and nature of the components of the active holoenzymes are as yet unknown.

In summary, POH can cause both apoptosis and cell cycle arrest both *in vivo* and *in vitro* (13). Interestingly, in certain *in vitro* systems POH preferentially induces either apoptosis or cell-cycle arrest. In the cell line studied here, the predominant effect of POH is cell-cycle arrest in G_1. This inhibition was associated with a reduction in both cyclin D- and E-associated kinase activities. The data may provide insight in exploring which tissues and tumor types are likely to respond to POH treatment in both cancer prevention and treatment applications. This could help direct future clinical trials.

Acknowledgements

The authors thank Ms Kathleen Schell, Kristin Elmer and Janet Lewis at the Flow Cytometry Facility, UW Comprehensive Cancer Center for technical assistance with flow cytometry experimentation and Dr Laurie A.Shepel for critical review of the manuscript. This work was supported in part by United States Public Health Service, National Institutes of Health Grant R37-CA38128.

References

1. Crowell,P.L. and Gould,M.N. (1994) Chemoprevention and therapy of cancer by D-limonene. *Crit. Rev. Oncogenesis*, **5**, 1–22.
2. Gould,M.N. (1997) Cancer chemoprevention and therapy by monoterpenes. *Environ. Health Perspect.*, **105** (suppl. 4), 977–979.
3. Vigushin,D.M., Poon,G.K., Boddy,A., English,J., Halbert,G.W., Pagonis,C., Jarman,M. and Coombes,R.C. (1998) Phase I and pharmacokinetic study of D-limonene in patients with advanced cancer. Cancer Research Campaign Phase I/II Clinical Trials Committee. *Cancer Chemother. Pharmacol.*, **42**, 111–117.
4. Ripple,G.H., Gould,M.N., Stewart,J.A., Tutsch,K.D., Arzoomanian,R.Z., Alberti,D., Feierabend,C., Pomplun,M., Wilding,G. and Bailey,H.H. (1998) Phase I clinical trial of perillyl alcohol administered daily. *Clin. Cancer Res.*, **4**, 1159–1164.
5. Ripple,G.H., Gould,M.N., Arzoomanian,R.Z. *et al.* (2000) Phase I clinical and pharmacokinetic study of perillyl alcohol administered four times a day. *Clin. Cancer Res.*, **6**, 390–396.
6. Maltzman,T.H., Christou,M., Gould,M.N. and Jefcoate,C.R. (1991) Effects of monoterpenoids on *in vivo* DMBA-DNA adduct formation and on phase I hepatic metabolizing enzymes. *Carcinogenesis*, **12**, 2081–2087.
7. Elson,C.E. and Yu,S.G. (1994) The chemoprevention of cancer by mevalonate-derived constituents of fruits and vegetables. *J. Nutr.*, **124**, 607–614.
8. Crowell,P.L., Chang,R.R., Ren,Z.B., Elson,C.E. and Gould,M.N. (1991) Selective inhibition of isoprenylation of 21–26-kDa proteins by the anticarcinogen D-limonene and its metabolites. *J. Biol. Chem.*, **266**, 17679–17685.
9. Schulz,S., Buhling,F. and Ansorge,S. (1994) Prenylated proteins and lymphocyte proliferation: inhibition by d-limonene related monoterpenes. *Eur. J. Immunol.*, **24**, 301–307.
10. Crowell,P.L., Ren,Z., Lin,S., Vedejs,E. and Gould,M.N. (1994) Structure–activity relationships among monoterpene inhibitors of protein isoprenylation and cell proliferation. *Biochem. Pharmacol.*, **47**, 1405–1415.
11. Ren,Z. and Gould,M.N. (1994) Inhibition of ubiquinone and cholesterol synthesis by the monoterpene perillyl alcohol. *Cancer Lett.*, **76**, 185–190.
12. Ariazi,E.A. and Gould,M.N. (1996) Identifying differential gene expression in monoterpene-treated mammary carcinomas using subtractive display. *J. Biol. Chem.*, **271**, 29286–29294.
13. Ariazi,E.A., Satomi,Y., Ellis,M.J., Haag,J.D., Shi,W., Sattler,C.A. and Gould,M.N. (1999) Activation of the transforming growth factor beta signaling pathway and induction of cytostasis and apoptosis in mammary carcinomas treated with the anticancer agent perillyl alcohol. *Cancer Res.*, **59**, 1917–1928.
14. Oka,Y., Rozek,L.M. and Czech,M.P. (1985) Direct demonstration of rapid insulin-like growth factor II receptor internalization and recycling in rat adipocytes. Insulin stimulates ^{125}I-insulin-like growth factor II degradation by modulating the IGF-II receptor recycling process. *J. Biol. Chem.*, **260**, 9435–9442.
15. Jirtle,R.L., Haag,J.D., Ariazi,E.A. and Gould,M.N. (1993) Increased mannose 6-phosphate/insulin-like growth factor II receptor and transforming growth factor beta 1 levels during monoterpene-induced regression of mammary tumors. *Cancer Res.*, **53**, 3849–3852.
16. Mills,J.J., Chari,R.S., Boyer,I.J., Gould,M.N. and Jirtle,R.L. (1995) Induction of apoptosis in liver tumors by the monoterpene perillyl alcohol. *Cancer Res.*, **55**, 979–983.
17. Reddy,B.S., Wang,C.X., Samaha,H., Lubet,R., Steele,V.E., Kelloff,G.J. and Rao,C.V. (1997) Chemoprevention of colon carcinogenesis by dietary perillyl alcohol. *Cancer Res.*, **57**, 420–425.
18. Sherr,C.J. (1996) Cancer cell cycles. *Science*, **274**, 1672–1677.
19. Weinberg,R.A. (1995) The retinoblastoma protein and cell cycle control. *Cell*, **81**, 323–330.
20. Nevins,J.R. (1992) E2F: a link between the Rb tumor suppressor protein and viral oncoproteins. *Science*, **258**, 424–429.
21. Dyson,N. (1998) The regulation of E2F by pRB family protein. *Genes Dev.*, **12**, 2245–2262.
22. Morgan,D.O. (1995) Principles of CDK regulation. *Nature*, **374**, 131–134.
23. Sherr,C.J. and Roberts,J.M. (1995) Inhibitors of mammalian G_1 cyclin-dependent kinases. *Genes Dev.*, **9**, 1149–1163.
24. Weinberg,R.A. (1991) Tumor suppressor genes. *Science*, **254**, 1138–1146.
25. Sherr,C.J. and Roberts,J.M. (1999) CDK inhibitors: positive and negative regulators of G_1-phase progression. *Genes Dev.*, **13**, 1501–1512.
26. LaBaer,J., Garrett,M.D., Stevenson,L.F., Slingerland,J.M., Sandhu,C., Chou,H.S., Fattaey,A. and Harlow,E. (1997) New functional activities for the p21 family of CDK inhibitors. *Genes Dev.*, **11**, 847–862.

27. Brugarolas,J., Bronson,R.T. and Jacks,T. (1998) p21 is a critical CDK2 regulator essential for proliferation control in Rb-deficient cells. *J. Cell Biol.*, **141**, 503–514.
28. Blain,S.W., Montalvo,E. and Massague,J. (1997) Differential interaction of the cyclin-dependent kinase (Cdk) inhibitor p27Kip1 with cyclin A–Cdk2 and cyclin D2–Cdk4. *J. Biol. Chem.*, **272**, 25863–25872.
29. Solomon,M.J. and Kaldis,P. (1998) Regulation of CDKs by phosphorylation. *Results Probl. Cell Differ.*, **22**, 79–109.
30. Aprelikova,O., Xiong,Y. and Liu,E.T. (1995) Both p16 and p21 families of cyclin-dependent kinase (CDK) inhibitors block the phosphorylation of cyclin-dependent kinases by the CDK-activating kinase. *J. Biol. Chem.*, **270**, 18195–18197.
31. Polyak,K., Lee,M.H., Erdjument-Bromage,H., Koff,A., Roberts,J.M., Tempst,P. and Massague,J. (1994) Cloning of p27Kip1, a cyclin-dependent kinase inhibitor and a potential mediator of extracellular antimitogenic signals. *Cell*, **78**, 59–66.
32. Medina,D., Kittrell,F.S., Liu,Y.J. and Schwartz,M. (1993) Morphological and functional properties of TM preneoplastic mammary outgrowths. *Cancer Res.*, **53**, 663–667.
33. Jerry,D.J., Medina,D. and Butel,J.S. (1994) p53 mutations in, D cells. *In vitro Cell. Dev. Biol.*, **30A**, 87–89.
34. Jenkins,C.W. and Xiong,Y. (1995) Immunoprecipitation and immunoblotting in cell cycle studies. In M. Pagano (ed.), *Cell Cycle: Materials and Methods.* Springer, New York, pp. 250–263.
35. Alpan,R.S. and Pardee,A.B. (1996) p21WAF1/CIP1/SDI1 is elevated through a p53-independent pathway by mimosine. *Cell Growth Differ.*, **7**, 893–901.
36. Lalande,M. (1990) A reversible arrest point in the late G1 phase of the mammalian cell cycle. *Exp. Cell Res.*, **186**, 332–339.
37. Watson,P.A., Hanauske-Abel,H.H., Flint,A. and Lalande,M. (1991) Mimosine reversibly arrests cell cycle progression at the G1–S phase border. *Cytometry*, **12**, 242–246.
38. Gu,Y., Rosenblatt,J. and Morgan,D.O. (1992) Cell cycle regulation of CDK2 activity by phosphorylation of Thr160 and Tyr15. *EMBO J.*, **11**, 3995–4005.
39. Said,T.K. and Medina,D. (1995) Cell cyclins and cyclin-dependent kinase activities in mouse mammary tumor development. *Carcinogenesis*, **16**, 821–830.
40. Haag,J.D. and Gould,M.N. (1994) Mammary carcinoma regression induced by perillyl alcohol, a hydroxylated analog of limonene. *Cancer Chemother. Pharmacol.*, **34**, 477–483.
41. Hitomi,M., Shu,J., Agarwal,M., Agarwal,A. and Stacey,D.W. (1998) p21Waf1 inhibits the activity of cyclin dependent kinase 2 by preventing its activating phosphorylation. *Oncogene*, **17**, 959–969.
42. Ren,Z., Elson,C.E. and Gould,M.N. (1997) Inhibition of type I and type II geranylgeranyl-protein transferases by the monoterpene perillyl alcohol in NIH3T3 cells. *Biochem. Pharmacol.*, **54**, 113–120.
43. Lee,S.J., Ha,M.J., Lee,J., Nguyen,P., Choi,Y.H., Pirnia,F., Kang,W.K., Wang,X.F., Kim,S.J. and Trepel,J.B. (1998) Inhibition of the 3-hydroxy-3-methylglutaryl-coenzyme A reductase pathway induces p53-independent transcriptional regulation of p21 (WAF1/CIP1) in human prostate carcinoma cells. *J. Biol. Chem.*, **273**, 10618–10621.
44. Vogt,A., Sun,J., Qian,Y., Hamilton,A.D. and Sebti,S.M. (1997) The geranylgeranyltransferase-I inhibitor GGTI-298 arrests human tumor cells in G0/G1 and induces p21 (WAF1/CIP1/SDI1) in a p53-independent manner. *J. Biol. Chem.*, **272**, 27224–27229.
45. Olson,M.F., Paterson,H.F. and Marshall,C.J. (1998) Signals from Ras and Rho GTPases interact to regulate expression of p21Waf1/Cip1. *Nature*, **394**, 295–299.
46. Adnane,J., Bizouarn,F.A., Qian,Y.M., Hamilton,A.D. and Sebti,S.M. (1998) p21 (WAF1/Cip1) is upregulated by the geranylgeranyltransferase inhibitor GGTI-298 through a transforming growth factor Beta- and Sp1-responsive element—involvment of the small GTPase RhoA. *Mol. Cell. Biol.*, **18**, 6962–6970.
47. Matsushime,H., Quelle,D.E., Shurtleff,S.A., Shibuya,M., Sherr,C.J. and Kato,J.Y. (1994) D-type cyclin-dependent kinase activity in mammalian cells. *Mol. Cell. Biol.*, **14**, 2066–2076.
48. Jinno,S., Hung,S.C. and Okayama,H. (1999) Cell cycle start from quiescence controlled by tyrosine phosphorylation of Cdk4. *Oncogene*, **18**, 565–571.
49. Terada,Y., Tatsuka,M., Jinno,S. and Okayama,H. (1995) Requirement for tyrosine phosphorylation of Cdk4 in G1 arrest induced by ultraviolet irradiation. *Nature*, **376**, 358–362.
50. Iavarone,A. and Massague,J. (1997) Repression of the CDK activator Cdc25A and cell-cycle arrest by cytokine TGF-beta in cells lacking the CDK inhibitor p15. *Nature*, **387**, 417–422.
51. Mahony,D., Parry,D.A. and Lees,E. (1998) Active cdk6 complexes are predominantly nuclear and represent only a minority of the cdk6 in T cells. *Oncogene*, **16**, 603–611.
52. Sweeney,K.J., Swarbrick,A., Sutherland,R.L. and Musgrove,E.A. (1998) Lack of relationship between CDK activity and G1 cyclin expression in breast cancer cells. *Oncogene*, **16**, 2865–2878.

Received January 9, 2001; revised August 20, 2001;
accepted September 18, 2001